J. Am. Chem. Soc. 102, 7126–7128.
Silverman, R. B., Hiebert, C. K., & Vazquez, M. L. (1985) *J. Biol. Chem.* (in press).
Tabor, C. W., Tabor, H., & Rosenthal, S. M. (1954) *J. Biol. Chem. 208*, 645–661.
Thomas, K. A., Smith, G. M., Thomas, T. B., & Feldmann, R. J. (1982) *Proc. Natl. Acad. Sci. U.S.A. 79*, 4843–4847.
Vazquez, M. L., & Silverman, R. B. (1985) *Biochemistry* (preceding paper in this issue).
Walsh, C. T. (1984) *Annu. Rev. Biochem. 53*, 493–535.
Winn, M., Horrom, B. W., Rasmussen, R. R., Chappell, E. G., & Plotnikoff, N. P. (1975) *J. Med. Chem. 18*, 437–438.
Zeller, E. A., Sarkar, S., & Reinene, R. M. (1962) *J. Biol. Chem. 237*, 2333–2336.

Kinetics of RNA Replication: Competition and Selection among Self-Replicating RNA Species[†]

Christof K. Biebricher and Manfred Eigen
Max-Planck-Institut für Biophysikalische Chemie, D-3400 Göttingen, Federal Republic of Germany
William C. Gardiner, Jr.*
Department of Chemistry, University of Texas, Austin, Texas 78712

Received January 7, 1985

ABSTRACT: The process of Darwinian selection in the self-replication of single-stranded RNA by Qβ replicase was investigated by analytical and computer-simulation methods. For this system, the relative population change of the competing species was found to be a useful definition of selection value, calculable from measurable kinetic parameters and concentrations of each species. Critical differences in the criteria for selection were shown to pertain for replicase/RNA ratios greater than or less than 1, for the case that formation of double-stranded RNA occurs and when comparisons are made of closed with open systems. At a large excess of enzyme, RNA species grow exponentially without interfering with each other, and selection depends only on the fecundity of the species, i.e., their overall replication rates. For RNA concentrations greater than the replicase concentration, the selection of species is governed by their abilities to compete for enzyme. Under conditions where formation of double strands occurs, competition leads to a coexistence of the species; the selection values vanish, and the concentration ratios depend only on the template binding and double-strand formation rates. The approach to coexistence is rapid, because when its competitors are in a steady state, a species present in trace amount is amplified exponentially. When formation of hybrid double strands occurs at a substantial rate, coexistence of hybridizing species is essentially limited to cases where the formation rate of heterologous double strands is smaller than the geometric mean of the formation rates of the homologous double strands. At limiting cases, e.g. in the steady states, simple analytical expressions for the main aspects of the selection process were found. Experimental data support the analytical expressions and the simulations.

Darwinian behavior, usually considered to be a characteristic of life itself, arises whenever a system has the characteristics of metabolism, self-reproduction, and mutability. It results in the production of species present in populations that depend on their "Darwinian fitness". The population changes of each species are functions not only of the prevailing conditions but also of the populations of all species present. It is thus not possible to derive selection values for species in an ecosystem from known characteristics of the species, e.g., fecundity, alone.

Laboratory studies of evolution at the molecular level were introduced in a classic series of experiments by Spiegelman and co-workers [Mills et al., 1967; reviewed by Biebricher (1983)] using RNA that was self-replicating in the presence of Qβ replicase. They showed that new RNA species can arise and outgrow other species. In a previous paper (Biebricher et al., 1983) we described an investigation of RNA replication kinetics by analytical and computer-simulation methods. A critical dependence on the RNA populations was found: Exponential growth occurs when enzyme is present in excess of RNA, while linear growth can occur when RNA is in excess. In a subsequent study (Biebricher et al., 1984), we explored the implications of two important features of RNA replication, the presence of two complementary RNA strand populations and their reaction with each other to form antiparallel double helices. The same methods are extended in this paper to considerations of the processes of competition and selection as they arise in laboratory studies of short single-stranded RNA replication by the enzyme Qβ replicase.

The primary results of the theoretical development are a demonstration that different selection criteria apply for competition between RNA species when the enzyme is saturated (RNA:enzyme ratio greater than 1) and when it is not (RNA:enzyme ratio less than 1) and that still different situations pertain when formation of double-stranded RNA proceeds in competition with recycling of single-stranded RNA template. For each of these situations, it was possible to derive analytical formulas epitomizing the selection criteria. Finally, distinctions are made between competition in closed systems and in open systems such as flow reactors or their discrete realizations as serial-transfer experiments.

[†] This research was carried out under the auspices of the Max-Planck-Gesellschaft. Additional support from the Alexander von Humboldt, Fritz Thyssen, and Robert Welch Foundations is also acknowledged.

0006-2960/85/0424-6550$01.50/0

MATERIALS AND METHODS

The mathematical approaches used for this investigation were the same as before (Biebricher et al., 1983, 1984). The computer simulations were done on the Univac 1100/83 of the Gesellschaft für Wissenschaftliche Datenverarbeitung, Göttingen, at an integration accuracy of $1/10^4$ or better.

The enzyme preparation method (Sumper & Luce, 1975), the determination of the rate constants in the linear and the exponential growth phases (Biebricher et al., 1981b), and the gel electrophoresis systems (Biebricher et al., 1982) were described previously.

RESULTS

Replication Mechanism. This study is based on the replication mechanism for single-stranded RNA shown in Figure 4 of Biebricher et al. (1983). We consider the population changes of species present in a sufficient number of copies to assure deterministic behavior. Asymmetry of kinetic parameters in the two complementary-strand cycles is neglected, as are species alterations by mutations. The effects of double-strand formation strongly influence the selection process (Biebricher et al., 1982) and cannot be neglected. They lead to a steady state of the concentrations of free template and free enzyme (Biebricher et al., 1984) and a linear formation rate of double-stranded RNA. Binding of double strands to enzyme is neglected also even though it has been found experimentally to occur (unpublished results); since dissociation of these complexes is rapid, the only effect is product inhibition by reversible binding of enzyme.

Simulations were always done with the complete mechanism [as described in Biebricher et al. (1983), Figure 4] assuming a chain length of 20 nucleotides. For analytical description of selection, a simplified three-step replication mechanism, wherein all elementary steps from geminal association to replica release are combined to a single "elongation step", was found to be appropriate. Additional reactions were included to describe homologous and hybrid double-strand formation. In contrast to the two-step replication mechanism used previously (Biebricher et al., 1984), this mechanism explicitly provides the correct enzyme dependence of the exponential growth rate, which is required for the analysis of competition. The simplified mechanism for replication of either strands of the ith RNA species is

$$^{i}\mathrm{I} + \mathrm{E} \xrightarrow{^{i}k_{\mathrm{A}3'}} {}^{i}_{1}\mathrm{IE}$$

$$^{i}_{1}\mathrm{IE} \xrightarrow{^{i}k_{\mathrm{E}}} {}^{i}\mathrm{I} + {}^{i}_{n}\mathrm{IE}$$

$$^{i}_{n}\mathrm{IE} \xrightarrow{^{i}k_{\mathrm{D}5'}} \mathrm{E} + {}^{i}\mathrm{I}$$

The prefixed superscript i denotes the ith RNA species, and the prefixed subscripts 1 and n denote 3′-bound and 5′-bound replication complexes as in the complete replication mechanism [Figure 4 and Table I of Biebricher et al. (1983)]. The 3′-association and 5′-dissociation steps are identified with actual elementary reactions, which for the RNA species that are studied under laboratory conditions are irreversible, while the many first-order steps involved in initiation of replication, chain elongation, and replica release are summarized as a single reaction and assigned an overall rate constant for elongation and replica release $^{i}k_{\mathrm{E}}$. For the usual laboratory conditions, 3′-association is a fast process determining the course but not the rate of replication, while elongation taking tens of seconds and 5′-dissociation taking hundreds of seconds determine the replication rate.

Homologous double-strand formation occurs without participation of enzyme by

$$^{i}\mathrm{I}^{+} + {}^{i}\mathrm{I}^{-} \rightarrow {}^{ii}\mathrm{II}$$

while hybridization between RNA species i and j includes the two possible elementary reactions:

$$^{i}\mathrm{I}^{+} + {}^{j}\mathrm{I}^{-} \xrightarrow{^{ij}k_{\mathrm{ds}}} {}^{ij}\mathrm{II} = {}^{ji}\mathrm{II} \xleftarrow{^{ji}k_{\mathrm{ds}}} {}^{i}\mathrm{I}^{-} + {}^{j}\mathrm{I}^{+}$$

While the two elementary reactions would in principle have independent hybridization rate constants and lead to two different hybrid double strands, considering a single hybrid captures the essential kinetic effects.

Selection Values. For study of competition, two replication cycles are considered, one for each RNA species. Enzyme, nucleoside triphosphate substrate, and inorganic pyrophosphate are the only reactants shared by the two cycles. In establishing a measure of the reaction rate in each cycle, it was useful to consider the amount of enzyme bound to each of the two RNA templates. We used as a key measure of RNA synthesis the rate of pyrophosphate (PP) production by nucleotide incorporation into each RNA species i, normalized for chain length n and for the total concentration of enzyme bound to that RNA species $[^{i}\mathrm{E_c}]$, and called it the turnover rate ρ:

$$^{i}\rho = \frac{\mathrm{d}[^{i}\mathrm{PP}]}{\mathrm{d}t} \frac{1}{(n-1)[^{i}\mathrm{E_c}]}$$

This expression becomes equal to $[^{i}\mathrm{E_c}]^{-1}\,\mathrm{d}[^{i}\mathrm{I}]/\mathrm{d}t$, where $[^{i}\mathrm{I}] = [^{i}\mathrm{I}^{+}] + [^{i}\mathrm{I}^{-}]$, for the case when double-strand formation is negligible and $2[^{i}\mathrm{E_c}]^{-1}\,\mathrm{d}[^{i}\mathrm{II}]/\mathrm{d}t$ when it is at steady state.

The selection parameters in use in population genetics pertain to sexually reproducing Mendelian populations and are not suitable for describing the RNA selection process. We found that the relative rate of population change of each active template is an appropriate measure of selection value (called $^{i}\sigma$) for the situation treated here:

$$^{i}\sigma = \frac{1}{[^{i}\mathrm{I}]} \frac{\mathrm{d}[^{i}\mathrm{I}]}{\mathrm{d}t}$$

The total RNA population becomes enriched in species with higher σ values and depleted in species with lower σ values. The selection values are not in general constant but functions of the concentrations of competitors; they often change significantly with time during a competition.

Competition in the Exponential Growth Phase. The simplest self-replicative competition arises when the constraints imposed upon the replication rate remain constant, such that the production rate of each RNA species is a function only of its own concentration (as far as mutational effects can be neglected). In such a situation, different RNA strands that may be present compete with one another without interacting with one another. The concentration sum of all forms of each species is much lower than the enzyme concentration and so low for each species that formation of double strands can be neglected. Exponential growth of all RNA species (including their replication intermediates) occurs. The selection values are then identical with the rates of exponential growth for each RNA species and independent of time and the concentrations of competitors. The kinetic equations reduce to the ones described in previous work (Biebricher et al., 1983, 1984) for exponential growth of single species. RNA species with slower replication rates are not suppressed by the faster species, but their proportion of the total RNA concentration declines steadily as the faster species outrace them. The situation has been realized experimentally by the serial dilution technique (Kramer et al., 1974) and discussed theoretically by Eigen

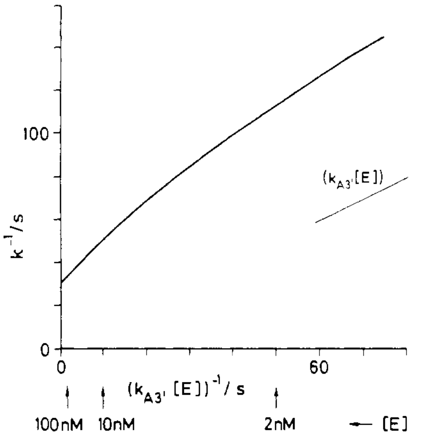

FIGURE 1: Lineweaver–Burk presentation for exponential growth phase of palindromic three-step replication mechanism. The enzyme concentrations shown are for $k_{A3'} = 10^7$ M^{-1} s^{-1} as in the standard rate constant set used in simulations. The low [E] limit expression (fine line) is not approached for the conditions of the simulations or the experiments.

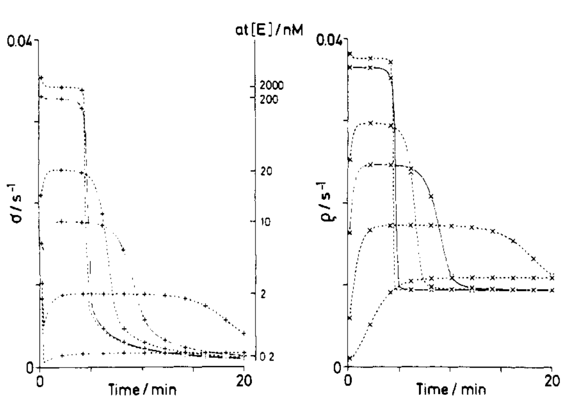

FIGURE 2: Computer simulations of the enzyme concentration dependence of the turnover rate ρ and the selection value σ. ρ and σ correspond to the overall rates measured experimentally in the linear and the exponential growth phases, respectively (Biebricher et al., 1981b). Simulations were done with standard rate constants (except for $k_{PI} = 0$) at enzyme concentrations [E] = 0.2, 2, 10, 20, 200, and 2000 nM as indicated. Note that in the linear growth phase ρ is constant and independent of [E] (the constant ρ value at [E] = 0.2 and 2 nM is reached at later times), while σ is constant in the exponential growth phase but independent of [E] only at saturating [E] values (>200 nM for the standard rate constant set).

Table I: Accuracy of Quadratic Approximation to Exponential Growth Equation for the Three-Step Replication Mechanism[a]

[E] (nM)	$10^3\kappa$ (cubic)	$10^3\kappa$ (quadratic)	$10^3\kappa$ (simulation)
1	5.8	5.8	5.8
2	8.9	9.1	8.9
5	14.5	14.9	14.6
10	19.5	20.0	19.3
20	24.3	24.9	23.9
∞	35.3	35.3	

[a] Standard set of rate constants. Units are s^{-1}.

(1971) and Eigen & Schuster (1977).

A fundamental conclusion of the cited theoretical work is that replacing an ordinary first-order growth process A → 2A with a self-replicative growth process $A^+ \rightarrow A^+ + A^-$ and $A^- \rightarrow A^- + A^+$ gives a coherent growth process in which, after a short relaxation time, the concentrations of both A^+ and A^- grow exponentially in time with the same exponential growth rate, such that their concentration ratio is constant. Analysis of the exponential growth kinetics for detailed RNA replication models showed that this basic picture is retained when the coherent growth process is decomposed into its elementary steps (Biebricher et al., 1983, 1984). Not only do both complementary template strands grow (after an initial equilibration period) in concentration with the same exponential time constant but so do all replication complexes involved. For the competition between two or more RNA species under pure exponential growth conditions, we confirmed by extensive simulations (an example is shown in the early time part of Figure 4) that only the overall growth constant of each complementary pair is important for determining the outcome of the selection process. Under exponential growth conditions, the outcome of the competition is selection of that species which has the maximum growth constant for the complementary pair under the selection conditions imposed.

In our previous work (Biebricher et al., 1983, 1984) it was of interest to examine the plus and minus replication cycles separately. Here our attention is focused on the competition between different RNA species; to simplify the equations, we will assume hereafter that the individual rate constants related to replication of the plus and minus strands of each species are the same, a simplification that we called in our previous work a palindromic mechanism. The designations $[^i\mathrm{I}]$, $[^i_1\mathrm{I}]$, and $[^i_n\mathrm{I}]$ are used to denote the total concentrations of each RNA and its two replication complexes, and the kinetic equations are developed accordingly. It was checked by computer simulations using different values for the rate constants for the replication of each strand that no essential features of competition and selection are lost by this simplifying assumption.

Solution of the kinetic equations for the palindromic three-step mechanism then requires finding the eigenvalues of a 3 × 3 rate constant matrix (Appendix I). The dependence of the exponential replication rate κ on the enzyme concentration was found to be quite complicated (Figures 1 and 2). For all conditions investigated experimentally, however, it was possible to reduce the formula for the exponential growth constant to a quadratic form that for enzyme concentrations over 100 nM (and the standard rate constant set) took on a form independent of enzyme concentration

$$\kappa = \frac{k_{DS'}}{2}\left[\left(1 + \frac{4k_E}{k_{DS'}}\right)^{1/2} - 1\right]$$

in agreement with experimental results (Biebricher et al., 1981b) and reminiscent of enzyme saturation similar to Michaelis–Menten behavior. The accuracy of the quadratic approximation is shown in Table I. In Figure 1 the enzyme concentration dependence is shown in a Lineweaver–Burk presentation, where a Michaelis–Menten-like near-linear form appears despite the apparent complexity of the formula. For the situation where replica elongation is very fast compared to template release, the high enzyme concentration limiting κ takes on the geometric mean form

$$\kappa = (k_E k_{DS'})^{1/2}$$

discussed in our earlier papers. If two competing RNAs are each at concentrations much lower than the enzyme concentration, then the outcome of the competition as long as this condition holds is determined fully by the two κ values, i.e., by the values of k_E and $k_{DS'}$ for each RNA species. If only one RNA species is at low concentration, then its growth rate depends on its κ value at the free enzyme concentration determined by the RNA species at higher concentration, a situation to which we return below.

Competition in the Linear Growth Phase. A linear increase in template RNA concentration occurs when the following

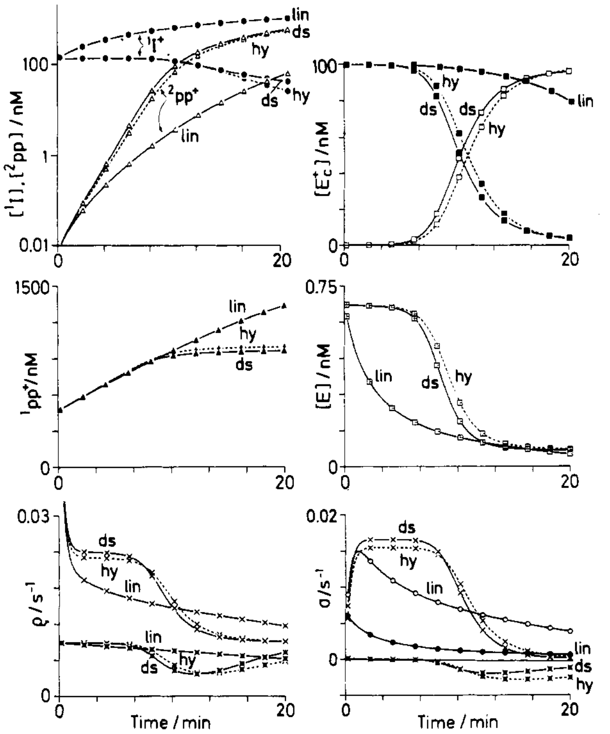

FIGURE 3: Competition and selection profiles under enzyme saturation conditions. Simulations were done with identical rate constants and starting concentrations for plus and minus strands. Concentrations shown here and in subsequent figures refer to plus strands only and are thus half of the total concentrations of each species. lin, linear growth phase, no double-strand formation; ds, double-strand formation at $^{11}k_{ds} = {}^{22}k_{ds} = 5 \times 10^4$ M^{-1} s^{-1}; hy, both double-strand formation at $^{11}k_{ds} = {}^{22}k_{ds} = 5 \times 10^4$ M^{-1} s^{-1} and hybridization at $^{12}k_{ds} = 2 \times 10^4$ M^{-1} s^{-1}. Otherwise, standard rate constant sets were used for both species except that $k_{PI} = 0$ and that new species (open symbols) has $^2k_{A3'} = 10 \times {}^1k_{A3'}$ (standard) $= 10^8$ M^{-1} s^{-1}. Substrate concentration was buffered at 500 μM; pyrophosphate concentration was buffered at 1 μM. Starting conditions: Double strand formation steady-state concentrations defined by double strand formation rate for the old species, and concentration of the new free RNA, $[^2I^+] = [^2I^-] = 10$ pM. Pyrophosphate concentrations (pp in figure) refer to the amounts generated by synthesis of each species separately and are normalized to the full-chain length through division by $(n - 1) = 19$. Hyperbolic decay of the free enzyme concentration [E] in the linear growth case retards the exponential outgrowth of the new species, expressing itself also (1) in the hyperbolic decays seen in the ρ and σ profiles for the linear growth case while plateaus pertain for double-strand formation and hybridization cases, (2) in the slower takeover of E_c by the new species in the linear growth case, and (3) in keeping the selective value of the old species $^1\sigma$ positive throughout. Double-strand formation causes the response of the free enzyme concentration to the selection process to appear as an adjustment from a higher to a lower value as the product of $k_{A3'}$ and the steady-state free RNA concentration adjusts to the final value.

conditions are fulfilled: (1) the enzyme is saturated with template, (2) reverse reactions such as pyrophosphorolysis or product inhibition by complexation at the replica site can be neglected, and (3) loss of template RNA by first-order (denaturation in closed systems or dilution in open systems) or second-order (formation of double-stranded RNA) processes does not occur. Once the steady state of replication under enzyme saturation conditions has been achieved, the behavior of the system fulfills, in a subtle and complex manner, the requirements for classical Michaelis–Menten enzyme catalysis. Again the replication rate (ρ) can be expressed in terms of elementary reaction rate constants, but the expression is quite different from that describing the exponential growth phase (Biebricher et al., 1983) and independent of the enzyme concentration (Figure 2). A steady-state equilibrium constant K_{IE} can be defined which for the case that enzyme reactivation is rate limiting takes a simple form:

$$K_{IE} = \frac{[E_c]}{[E][I]} = k_{A3'}\frac{k_E + k_{D5'}}{k_E k_{D5'}} \rightarrow \frac{k_{A3'}}{k_{D5'}}$$

The enzyme concentration

$$[E] = \frac{k_{D5'}[E_c]}{k_{A3'}[I]} = \frac{\rho}{k_{A3'}[I]} = \frac{\sigma}{k_{A3'}}$$

steadily decreases as the RNA concentration grows, a linear increase of [I] resulting in a hyperbolic decrease in [E] (Figure 3). A new mutant present in very small concentration (much below the free enzyme concentration) grows with an exponential rate κ corresponding to this enzyme concentration. The Lineweaver–Burk representation of $[E]^{-1}$ vs. κ^{-1} (Figure 1) shows that the assumption of a linear relationship between these two values would not give much error, so that σ for a new mutant would also fall hyperbolically.

It should be emphasized that this behavior of [E] is limited to the situation in a closed system, where the only source of free enzyme is through dissociation of the 5′-bound complex. In a flow system where free enzyme is supplied in the input flow (Appendix II), a constant and for all practical situations much higher value of [E] is maintained. In the closed system, the outcome of a competition between two RNA species in the linear growth phase depends on how well each competes with the other for the free enzyme that becomes available upon release of 5′-bound template from the replication complex. The selection pace, however, is determined by the overall replication rates of the competitors, because the competition is only for free enzyme as it is released from the linearly growing prevalent RNA and the (approximately exponential) rate of growth of the low-concentration competitor. A simulation (using the complete mechanism) illustrating the course of such a selection process is shown in Figure 3.

Competition at Double Strand Formation Steady State. The concentration of complementary free templates may become high enough that formation of double strands cannot be neglected. For most species that have been studied so far, double-strand formation already becomes noticeable at the onset of the linear growth phase, as shown in Figure 4. Since the double strand is inactive as template (although it does have a finite binding constant to enzyme), its formation acts as a sink for template. Continued RNA synthesis eventually leads to a steady state in which the rates of synthesis and double-strand formation are equal (Biebricher et al., 1984).

Let us consider first the case that double-strand formation among plus and minus strands of the same species occurs but hybridization among different species can be neglected. Free single strands, all intermediates, and the free enzyme then attain steady-state concentrations. The selection value of the species is thus zero under steady-state conditions, while the double-strand concentration grows linearly at half the turnover rate ρ according to

$$d[II]/dt = \rho[E_c]/2 = v/2$$

A new species arising spontaneously or introduced artificially in the steady state of the old species is presumably in very low concentration. Its double strand formation rate can be neglected, and it will grow exponentially with a rate corresponding to the steady-state free-enzyme concentration. After its concentration exceeds the free-enzyme concentration, it continues to grow with a declining rate as it competes with the old species for free enzyme (Figure 5). The $[E_c]$ and [I] values of the old species thus decrease, and its selection value goes through negative values until a new steady state with a

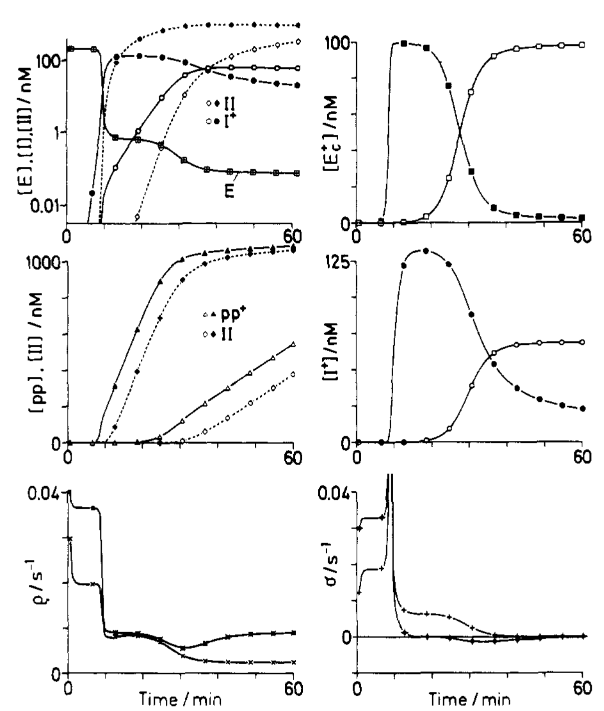

FIGURE 4: Effects of $k_{A3'}$ and $k_{D5'}$ in exponential growth and double strand formation steady state, illustrating the difference in selection criteria for different replication phases. Solid symbols, species 1; open symbols, species 2. Standard set was used except ${}^2k_{A3'} = 4 \times {}^1k_{A3'} = 4 \times 10^7\ M^{-1}\ s^{-1}$, ${}^2k_{D5'} = (1/4){}^1k_{D5'} = 2.5 \times 10^{-3}\ s^{-1}$, and ${}^{11}k_{ds} = {}^{22}k_{ds} = 10^4\ M^{-1}\ s^{-1}$. Starting conditions were [E] = 200 nM and $[{}^1I^+] = [{}^1I^-] = [{}^2I^+] = [{}^2I^-] = 1$ pM. The free enzyme concentration drops twice as each species approaches its double strand formation steady state. The first of these generates a kink in the growth profiles of RNA and pyrophosphate concentrations, resulting in rapid drops in ρ and σ for both species. The factors of 4 differences in rate constants generate factors of 1, 2, and 4 differences in rates and factors of 2 and 16 differences in concentrations (see Appendixes I and IV). The spikes in ${}^1\sigma$ and ${}^2\sigma$ arise during the transition from exponential growth of both species to exponential growth of one species (at a lower enzyme concentration) while the other is already at a double strand formation steady state. They are caused by the fact that free RNA is temporarily still being produced at the increasing rate characteristic of the exponential growth phase while the free enzyme concentration available to form replication complexes with it is dropping rapidly from its initial value.

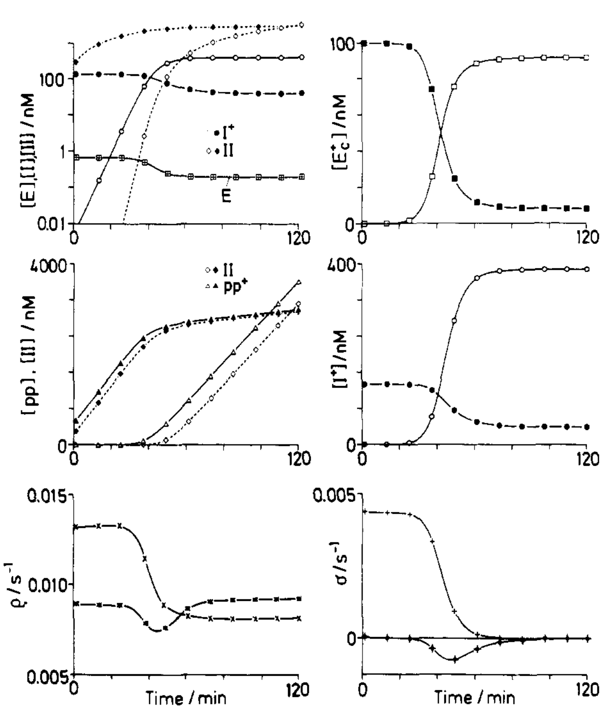

FIGURE 5: Replacement of one double strand formation steady state by another after exponential growth of a new species (open symbols). Rate constant set for old species 1 (solid symbols) is the standard set except ${}^1k_{PI} = 2 \times 10^5\ M^{-1}\ s^{-1}$ and ${}^{11}k_{ds} = 5 \times 10^4\ M^{-1}\ s^{-1}$; rate constant set for new species 2 is the standard set except ${}^2k_{PI} = 2 \times 10^5\ M^{-1}\ s^{-1}$ and ${}^{22}k_{ds} = 5 \times 10^3\ M^{-1}\ s^{-1}$. Starting conditions were double strand formation steady state of old species, concentration of new species $[{}^2I^+] = [{}^2I^-] = 7.5$ pM, and substrate concentration buffered at 500 μM. Establishment of the coexistence concentrations is accompanied by adjustment of the rates ρ to new stationary values while both selective values σ approach zero. The different values of ρ in the coexistence phase arise because the different [E$_c$] values imply different amounts of product inhibition for the two species.

lower free-enzyme concentration is reached, where both species have achieved their steady-state values and coexist. At this stage, the selection values of both species vanish.

The final steady-state concentrations can be described in relatively simple terms (Appendix IV). This is illustrated by the ratio of free RNA concentrations

$$\frac{[{}^2I]}{[{}^1I]} = \frac{{}^2k_{A3'}{}^{11}k_{ds}}{{}^1k_{A3'}{}^{22}k_{ds}}$$

The concentrations of each of the two double-stranded species grow as the squares of the single strands, as given by the constant ratio

$$\frac{d[{}^{22}II]/dt}{d[{}^{11}II]/dt} = \frac{{}^2\rho}{{}^1\rho} = \frac{({}^2k_{A3'})^2({}^{11}k_{ds})}{({}^1k_{A3'})^2({}^{22}k_{ds})}$$

Simulations showing the competition between two species that can form double strands are shown in Figures 4 and 5. They confirm that the ratio of 3′-association and double strand formation rate determine the concentration ratio of different species.

If the two species have related nucleotide sequences, the formation of mixed double strands ("hybrids") must also be taken into account. In the case where the two species are members of the same quasispecies distribution, the formation rate of mixed double strands usually equals that of homologous double strands. This reaction cannot be neglected when a new mutant is growing out in the steady state of the wild type, since the free template concentration of the latter species may be quite high. When hybridization does occur, coexistence of two species is restricted (Appendix V). It is required that the rate constant for double-strand formation between the competing species ${}^{12}k_{ds}$ be less than the geometric mean of the rate constants for complementary double-strand formation:

$${}^{11}k_{ds}{}^{22}k_{ds} > ({}^{12}k_{ds})^2$$

A further condition is that a certain combination of association and double-strand formation rate constants must lie within this range:

$${}^{11}k_{ds}{}^{22}k_{ds} > \frac{{}^{22}k_{ds}{}^{12}k_{ds}{}^1k_{A3'}}{{}^2k_{A3'}} > ({}^{12}k_{ds})^2$$

Only if these inequalities are satisfied does coexistence of two competing species occur. Species 1 is the predominant one if the following expression is positive:

$$\frac{{}^1k_{A3'}}{{}^2k_{A3'}} - \frac{1 + {}^{11}k_{ds}/{}^{12}k_{ds}}{1 + {}^{22}k_{ds}/{}^{12}k_{ds}}$$

It is characteristic of both the simple double strand formation and hybridization steady states that two (or more) competing species may coexist, with enzyme and single-strand concentrations held at constant values determined by the rate constants, and that constant growth rates of the double strands may be attained. A new feature of the hybridization case is

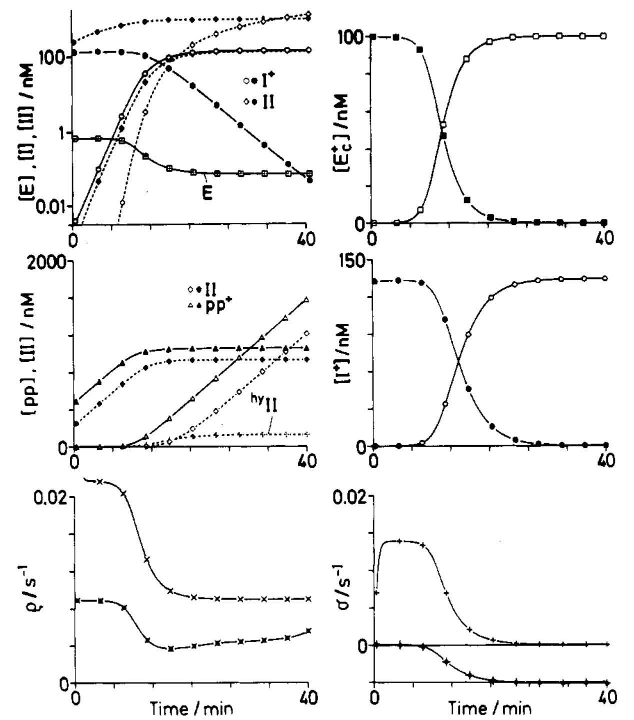

FIGURE 6: Destruction of an old species (solid symbols) and outgrowth of a new species (open symbols) through hybridization. Rate constants and starting conditions are as in the hy case of Figure 3 except $^{12}k_{\mathrm{ds}} = 5 \times 10^4$ M^{-1} s^{-1} and $[^2\mathrm{I}^+] = [^2\mathrm{I}^-] = 7.5$ pM. Note the adjustment of [E] to a lower steady-state concentration and the exponential decay of [^{1}I] (and thus negative $^2\sigma$) as the second species takes over the enzyme.

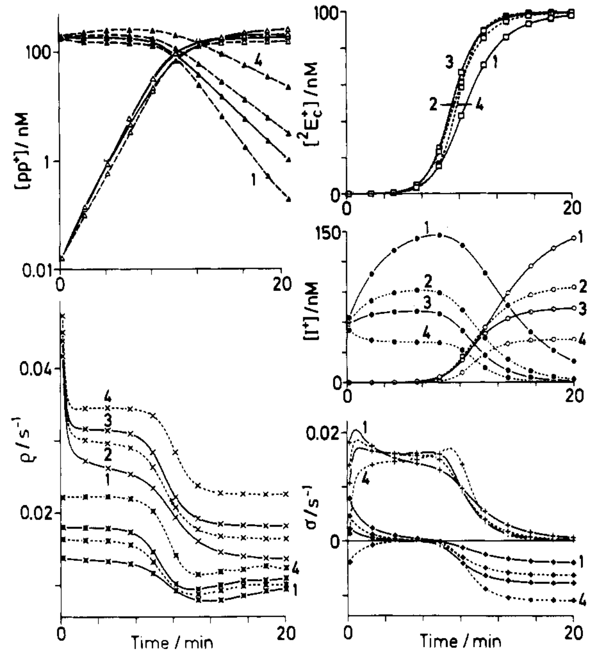

FIGURE 7: Effect of flow rate on selection under enzyme saturation conditions without formation of double strands. Rate constants and starting conditions as in the lin case of Figure 3 except $^1k_{\mathrm{PI}} = {}^2k_{\mathrm{PI}} = 2 \times 10^5$ M^{-1} s^{-1}. The values of k_{DIL} were 0.5×10^{-2}, 0.8×10^{-2}, 1.0×10^{-2}, and 1.5×10^{-2} s^{-1} for curves 1–4, respectively. Both the growth of the new species 2 (open symbols) and the washout of the old species 1 (solid symbols) appear as exponential profiles. While the rate profiles ρ remain positive for both species, the selective values $^1\sigma$ for the old species go negative and those of the new species $^2\sigma$ go to zero as the flow steady state is established.

the forced extinction of the weaker competitor when the above coexistence criteria are not satisfied (Figure 6).

Competition in Open Systems. In vitro selection experiments can be carried out under conditions such that a fresh supply of nucleoside triphosphates and replicase is maintained. The original method for achieving this involved periodic transfer of aliquots of an incubation mixture to fresh incubation medium (Kramer et al., 1974). A continuous-flow alternative would be to keep the incubation mixture refreshed by a steady flow of reagents (Eigen & Winkler-Oswatitsch, 1973, 1975; Küppers, 1979). These two alternative realizations of evolution in open systems were simulated in the computer model in two ways. The first was by periodic multiplication of all concentrations by a dilution factor, followed by readjustment of reagent concentrations, and the second by adding dilution terms to the set of differential equations used for closed-system simulations (Appendix II). The results of the open-system simulations were quite different for the three replication phases.

For replication in the exponential phase, the only difference noted was the trivial one that a species whose growth rate is less than the dilution rate dies out with first-order kinetics at a rate given by the difference between the growth and dilution rate constants. The nature and time scale of the competition are unaffected. Under enzyme saturation conditions, however, an essential new factor is introduced in the open system: free enzyme becomes available to the replication process by a new route besides dissociation of 5′-bound replication complexes. Depending upon the flow or serial-transfer conditions, supply of free enzyme in an open system by influx of fresh reagent may even be the predominant source that needs to be considered for the course of competition and selection.

In Figure 7 are shown several sets of profiles at varying flow rates, illustrating the takeover of an old species in the linear growth phase by a stronger competitor. The corresponding equations for the three-step mechanism (Appendix II), which are confirmed by simulations to be accurate for the rate constants used, show that only the free template concentration depends upon the input enzyme concentration [E$_{\mathrm{in}}$]. All other concentrations depend on rate constants only.

The experimentally interesting case that double-strand formation and flow both provide loss terms was also investigated by simulations. It was found that a smooth transition from the pure flow to the pure double strand formation cases exists. The analytic equations for the three-step mechanism can be derived (Appendix II), but for the interesting case where flow and double strand formation losses are comparable the equations are too complicated to be informative.

Laboratory Selection Experiments. The first important principle of selection among competing RNA species is the distinction between the selection criteria in the exponential and linear growth phases. The growth phase can be maintained by use of the technique of serial transfers (Kramer et al., 1974). In order to interpret the selection criteria correctly, it is necessary to adjust the transfer incubation time t_{tr} and the dilution factor F_{DIL} of each transfer in such a way that the selection conditions are kept constant.

In the exponential growth phase, the total concentration of each species at transfer $n + 1$ is

$$[{}^i\mathrm{I}_0]_{n+1} = ([{}^i\mathrm{I}_0]_n/F_{\mathrm{DIL}}) \exp({}^i\kappa t_{\mathrm{tr}}) = [{}^i\mathrm{I}_0]_n \exp[({}^i\kappa - \varphi)t_{\mathrm{tr}}]$$

where $\varphi = \ln (F_{\mathrm{DIL}})/t_{\mathrm{tr}}$. In a mixture of different species, the concentrations of species with ${}^i\kappa < \varphi$ decrease while the concentrations of species with ${}^i\kappa > \varphi$ increase. In Figure 8 the evolution of an RNA species starting with a de novo RNA is shown. (Care was taken that the RNA concentration did not increase to values reaching the enzyme concentration.) In this experiment φ was 2.3×10^{-2} s^{-1}, and the ${}^i\kappa$ values of species

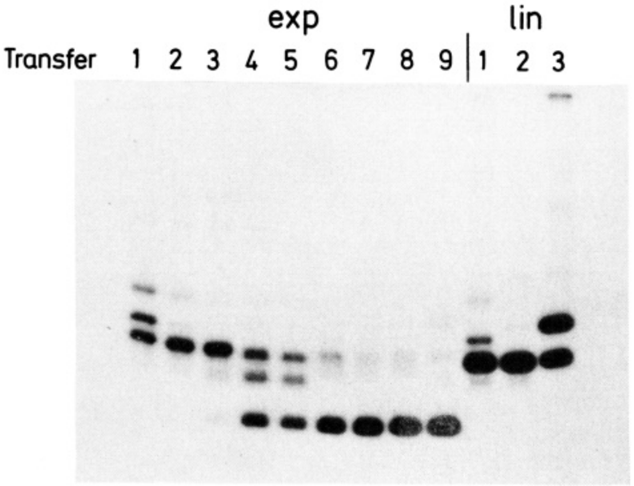

FIGURE 8: Selection of new RNA species in the exponential and in the linear phase. The reaction mixture contained 0.05 M Tris-HCl buffer (pH 7.5), 10 mM $MgCl_2$, 300 μM each of CTP, GTP, and UTP, 150 μM [α-^{32}P]ATP (sp act. 100 Ci/mol), and 140 nM holo-Qβ replicase. For transfers in the exponential phase, 20-μL samples were started with 1 μL of a 1:50 dilution of the previous transfer (total dilution 1:1000). After 5 min at 30 °C, a 5-μL aliquot was withdrawn and diluted 1:50 for the next transfer; after 15 min further incubation to allow sufficient synthesis, the sample was frozen prior to loading on the gel. For transfers in the linear phase, 20-μL samples were started with 1 μL of the previous transfer and incubated for 2, 2, and 15 h for the three transfers. As template in the first transfer a de novo product (Biebricher et al., 1981a) was used. The positions of the synthesized bands were determined by autoradiography. Enzyme saturation was reached within the last minute of transfer, causing an additional selection pressure.

that grew out had to be larger than this value.

As seen in Figure 8, experiments with serial transfers in the linear phase can exhibit quite different selection pressures. For transfers in the linear phase, low dilution factors and long incorporation times are required. For the transfer conditions used, the competing species usually reached their steady states of double-strand formation. Serial transfers in the linear phase are also complicated by product inhibition, which was neglected in the simplified theoretical treatment. Furthermore, the steady-state concentrations of single-stranded template were usually too low to saturate the enzyme after the transfer, and a short exponential amplification thus occurred at the beginning of each transfer. Under these conditions, the selection behavior was complicated, the total RNA concentration at the start of the next transfer being $[{}^i\mathrm{I}_0]_{n+1} = ([{}^i\mathrm{I}_0]_n/F_{\mathrm{DIL}}) + \int [{}^i\mathrm{I}_0]{}^i\sigma \, dt$, where ${}^i\sigma$ is not independent of time. (The selective value ${}^i\sigma$, defined as the logarithmic time derivative of the free RNA concentration alone, is also the logarithmic derivative of the total RNA concentration in both the exponential and the linear growth phases. In the exponential phase they are equal because of the coherent growth process, and in the linear phase they are equal because the bound RNA concentration remains constant.) The evaluation of the species concentrations in the electrophoresis gels was further complicated because usually only double strands can be observed on the gel, the proportion of single strands being too low to detect. In agreement with the theoretical results we found (1) sudden appearance of new species taking over, the concentration ratio between the active intermediates of two species changing between single transfers by as much as 8 orders of magnitude (Biebricher, 1983), and (2) often a coexistence of two species, so that further transfers effect no further increase in the proportion of an apparently superior species.

Table II: Replication Rates of MNV-11 and MDV-1[a]

species	κ (10^{-2} s^{-1})	ρ (10^{-3} s^{-1})	$\tau_D = 1/k_{DS'}$ (s)	$\tau_E = 1/k_E$ (s)
MNV-11	1.9	6.4	140	14
MDV-1	1.4	3.6	260	15

[a] The κ and ρ values of MNV-11 and MDV-1 were determined under the conditions used for the competition experiment shown in Figure 9 by the method described previously (Biebricher et al., 1981b). The retention times for enzyme reactivation and elongation were calculated from κ and ρ by the formulas in Appendix I.

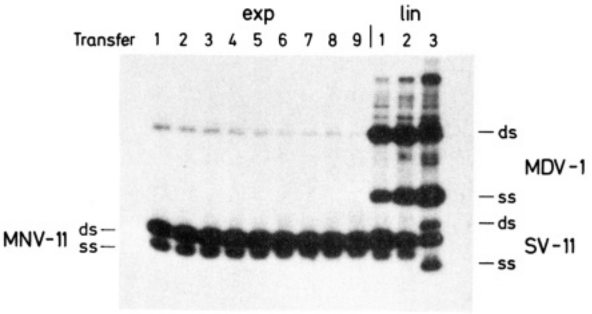

FIGURE 9: Competition of MNV-11 and MDV-1 in the exponential and the linear growth phases. The reaction mixture and the procedure were as described in Figure 8, except that the first transfer was started with equimolar amounts of single-stranded MNV-11 and MDV-1 and that incubation in the exponential phase was for 7 min at 30 °C. The SV-11 species appearing as a competitor at the third transfer in the linear phase is a close relative of MNV-11 (Biebricher et al., 1982). Under these conditions, enzyme saturation was reached during the transfer. With incubation times reduced to 6 min (not shown), the MNV-11 band remained constant, but the MDV-1 band had vanished after the second transfer.

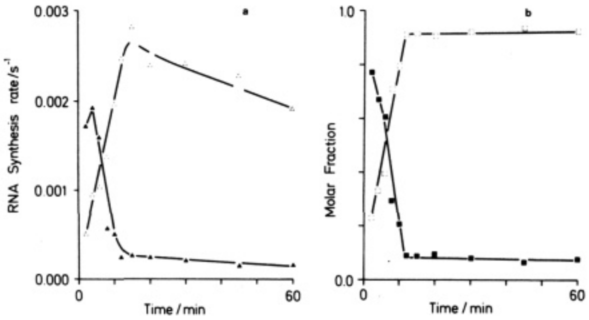

FIGURE 10: Takeover of enzyme by MDV-1 RNA in a linearly growing MNV-11 culture. The reaction mixture (200 μL) concentrations were 50 mM Tris-HCl buffer (pH 7.5), 10 mM $MgCl_2$, 50 mM $(NH_4)_2SO_4$, 300 μM each of CTP, GTP, and UTP, 150 μM ATP, and 140 nM holo-Qβ replicase. Synthesis was started with addition of ss-MNV-11 (50 nM). After 10-min incubation at 30 °C, ss-MDV-1 was added (1.4 nM) and the incubation continued. At the indicated times, 20 μL of the mixture was pipetted into a test tube containing 1 μCi of [α-^{32}P]ATP; after 8-min incubation, the test tubes were quickly frozen to quench the reaction. MDV-1 and MNV-11 were separated by electrophoresis, the bands were cut out, and the radioactivity was determined. (a) Synthesis rates of MNV-11 (filled symbols) and MDV-1 (open symbols); (b) proportion of the radioactivity incorporated into each species.

These effects were investigated in detail by competition between two well-characterized species, e.g., MNV-11 and MDV-1. The results are illustrated in Table II and Figures 9 and 10. In both growth phases, MNV-11 grew faster, because it had a substantially higher enzyme reactivation rate. In the exponential phase, the expected behavior was found: MNV-11 won the competition. If the dilution rate φ was chosen to equal the κ value of MNV-11, the MNV-11 concentration remained constant while the MDV-1 concentration decreased. After a sufficient number of transfers, it could be shown that MDV-1 had been diluted out and could not be detected any more in the RNA population. In the linear phase, on the other hand, MDV-1 rapidly overtook MNV-11 despite its lower replication rate. The takeover is illustrated in Figure 10. MNV-11 was first replicated until the steady state of double-strand formation was reached (after about 10 min); MDV-1 RNA was then added at a concentration of $[\text{E}_0]/100$. Labeling for 8 min at different growth times and measuring the synthesized amount of each species gave the v values. Since ρ was known for each species (Table II), the ratio ${}^iv/{}^i\rho$ yielded values for the concentrations $[{}^i\text{E}_\text{c}]$. As seen, MDV-1 robbed MNV-11 of most of its enzyme; however, a steady state was reached where MNV-11 remained at a low but constant level. The low steady-state concentration of MNV-11 could be measured conveniently by its preferential amplification in the exponential growth phase; it was found to be impossible to reduce the proportion of MNV-11 by further transfers in the linear phase. The results obtained in the experimental work resembled strikingly the simulation shown in Figure 4.

It was known from earlier work that the double strand formation rate of MDV-1 is substantially lower than that of MNV-11 (Biebricher et al., 1982). Hybridization between MNV-11 and MDV-1 was not observed (results not shown). An answer to the question of whether the difference in k_ds alone is sufficient to explain the selection advantage of MDV-1 in the linear phase, however, must await quantitative measurement of the k_ds and $k_{\text{A}3'}$ values of the corresponding species. Simulations alone cannot clarify it, since a selective advantage of the more slowly growing mutant by a higher template binding rate or a lower rate of double-strand formation would give very similar profiles (compare Figures 4 and 5).

The rate of RNA replication was always found to decrease steadily after the enzyme became saturated with template (Figure 10a). This is due to a product inhibition route neglected in the simulations shown. Introducing the rates (estimated from filter binding experiments) for the reversible binding of double strands to free enzyme into the simulation produced similar declines of $[{}^i\text{E}_\text{c}]$ with increasing concentrations of double strand. This accounts for the decline of the v values in the linear growth phase while the ρ values remain constant.

DISCUSSION

The results show that competition in the exponential and the linear growth phases follows two fundamentally different principles, the first being selection for fecundity and the latter being selection for displacement. The selection criteria are therefore quite different in each phase. In earlier evolution experiments, this difference has not been noted, and no care was therefore taken to ensure constant selection criteria. While selection in the exponential growth phase has been correctly described previously (Eigen, 1971; Kramer et al., 1974; Batschelet et al., 1976), it had been generally extrapolated to the linear phase on the assumption that one only had to consider that growth is braked at the onset of the linear phase (Kramer et al., 1974).

While in the exponential growth phase many replication rounds are necessary for selection unless there are extreme differences in the growth rates, very rapid selection of new species with similar growth rates was observed in the linear growth phase (Biebricher et al., 1982). An even more surprising result was that often the more slowly replicating species was selected. These results are now fully understandable: new species can grow up exponentially over several orders of magnitudes while the old wild type approaches or has already reached its steady-state concentration. Furthermore, in most cases the shorter species is selected in the exponential growth phase while the larger species wins in the linear growth phase. Kinetic analysis indicated a correlation of higher chain length with a slower enzyme reactivation rate and a lower rate of double-strand formation. Assuming similar tertiary structures of the RNA species, the double strand formation rate would be expected to be inversely proportional to the square root of the chain length (Wetmur & Davidson, 1968), which we did not find to be the case. The more stable secondary structure of the longer species (Biebricher et al., 1982) seems to account more for reducing the rate of double-strand formation. The rate of double-strand formation also shows a marked salt effect (Wetmur & Davidson, 1968), because the reaction involves two strongly negatively charged chains. Indeed, at higher ionic strength the selection pressure for a lower double strand formation rate was found to be much higher.

Other experimental phenomena are also easily explained. MCV-1 was found consistently to contaminate MDV-1 preparations even though their nucleotide sequences appear to be unrelated (Mills et al., 1975). This phenomenon is apparently an example of a coexistence of species in the steady state of double-strand formation. Other examples of coexistence may be masked by the large predominance of one species over the other; the presence of small amounts of MNV-11 in the coexistence steady state of MDV-1 and MNV-11 is not detected on normal gels.

The analysis given in this paper neglected the interconversion of species by mutations. If they are considered, the growth of the members of a quasi-species population is described (Eigen, 1971; Eigen & Schuster, 1977) by a set of differential equations of the form

$$x_i = (w_{ii} - \bar{E})x_i + \sum_{k\neq i} w_{ik}x_k$$

Here, x_i is the relative population of species i, i.e., $x_i = [{}^i\text{I}]/\sum[{}^ki]$, and w_{ii} is the growth rate $A_iQ_i - D_i$, the replication rate A_i producing a fraction Q_i of correct copies decaying with the first-order rate D_i, and $\bar{E}$ is the average excess production rate of the distribution, which can be found by summing over all species. In the present analysis, Q_i is assumed to be 1, and the w_{ik} terms are assumed to be zero, so that w_{ii} in the above equation is then equivalent to the selection value σ discussed in this work. The results of this paper can be expected to have important implications for the quasi-species distribution. It can be predicted that the mutant distribution changes after transition from exponential to linear growth. At the steady state of double-strand formation, coexistence requires a lower formation rate of hybrid double strands than of homologous strands, which is unlikely for point mutations. For the case of identical rate constant values for formation of mixed and homologous double strands, simulations have shown that mutants that may be present grow concomitantly with the wild type unless their template binding or double strand formation rates differ. In other words, at the steady state of double-strand formation, mutants with faster or slower growth due to elongation or enzyme reactivation rates all have selection values of zero, and their representation in the quasi-species neither increases nor decreases. Mutations involving rearrangements of the sequence, on the other hand, produce species with low rates of hybridization, and those mutants can multiply rapidly and capture a substantial proportion of the enzyme. Confirmation of these predictions, however, must await experimental determination of the mutant spectrum of the quasi-species.

APPENDIX

(*I*) *Summary of Kinetics for Three-Step Palindromic Replication Mechanism without Double-Strand Formation or Flow Losses*

The reaction mechanism is

$$\mathrm{I}^+ + \mathrm{E} \rightarrow {}_1\mathrm{I}^+\mathrm{E} \qquad k_{\mathrm{A3'}}\ (10^7\ \mathrm{M}^{-1}\ \mathrm{s}^{-1}\ \mathrm{std})$$

$${}_1\mathrm{I}^+\mathrm{E} \rightarrow {}_n\mathrm{I}^+\mathrm{E} + \mathrm{I}^- \qquad k_{\mathrm{E}}\ (16 \times 10^{-2}\ \mathrm{s}^{-1}\ \mathrm{std})$$

$${}_n\mathrm{I}^+\mathrm{E} \rightarrow \mathrm{E} + \mathrm{I}^+ \qquad k_{\mathrm{D5'}}\ (10^{-2}\ \mathrm{s}^{-1}\ \mathrm{std})$$

and similarly for the minus strand. We define the sum concentrations $[\mathrm{I}] = [\mathrm{I}^+] + [\mathrm{I}^-]$, $[{}_1\mathrm{IE}] = [{}_1\mathrm{I}^+\mathrm{E}] + [{}_1\mathrm{I}^-\mathrm{E}]$, $[{}_n\mathrm{IE}] = [{}_n\mathrm{I}^+\mathrm{E}] + [{}_n\mathrm{I}^-\mathrm{E}]$, $[\mathrm{E_c}] = [{}_1\mathrm{IE}] + [{}_n\mathrm{IE}]$, $[\mathrm{I_0}] = [\mathrm{I}] + [\mathrm{E_c}]$, and $[\mathrm{E_0}] = [\mathrm{E}] + [\mathrm{E_c}]$ and the expression

$$K_{\mathrm{IE}} = [\mathrm{E_c}]/([\mathrm{I}][\mathrm{E}])$$

The kinetic equations are

$$\frac{\mathrm{d}[\mathrm{I}]}{\mathrm{d}t} = -k_{\mathrm{A3'}}[\mathrm{E}][\mathrm{I}] + k_{\mathrm{E}}[{}_1\mathrm{IE}] + k_{\mathrm{D5'}}[{}_n\mathrm{IE}]$$

$$\frac{\mathrm{d}[{}_1\mathrm{IE}]}{\mathrm{d}t} = k_{\mathrm{A3'}}[\mathrm{E}][\mathrm{I}] - k_{\mathrm{E}}[{}_1\mathrm{IE}]$$

$$\frac{\mathrm{d}[{}_n\mathrm{IE}]}{\mathrm{d}t} = k_{\mathrm{E}}[{}_1\mathrm{IE}] - k_{\mathrm{D5'}}[{}_n\mathrm{IE}]$$

$$\frac{\mathrm{d}[\mathrm{I_0}]}{\mathrm{d}t} = k_{\mathrm{E}}[{}_1\mathrm{IE}]$$

Steady-State Solution. Setting $\mathrm{d}[{}_1\mathrm{IE}]/\mathrm{d}t = \mathrm{d}[{}_n\mathrm{IE}]/\mathrm{d}t = 0$ and using $[\mathrm{E_0}]$ = constant give

$$\frac{\mathrm{d}[\mathrm{I}]}{\mathrm{d}t} = \frac{v_{\max}[\mathrm{I}]}{K_{\mathrm{IE}}^{-1} + [\mathrm{I}]}$$

$$v_{\max} = \frac{k_{\mathrm{E}}k_{\mathrm{D5'}}}{k_{\mathrm{E}} + k_{\mathrm{D5'}}}[\mathrm{E_0}] = k_{\mathrm{A3'}}[\mathrm{E_0}]/K_{\mathrm{IE}}$$

$$K_{\mathrm{IE}} = \frac{k_{\mathrm{A3'}}(k_{\mathrm{E}} + k_{\mathrm{D5'}})}{k_{\mathrm{E}}k_{\mathrm{D5'}}} \qquad [\mathrm{E}] = \frac{[\mathrm{E_0}]}{1 + [\mathrm{I}]K_{\mathrm{IE}}}$$

$$[\mathrm{E_c}] = \frac{[\mathrm{E_0}][\mathrm{I}]}{K_{\mathrm{IE}}^{-1} + [\mathrm{I}]} \qquad \rho = \frac{1}{[\mathrm{E_c}]}\frac{\mathrm{d}[\mathrm{I}]}{\mathrm{d}t} = \frac{k_{\mathrm{A3'}}}{K_{\mathrm{IE}}} = \frac{k_{\mathrm{E}}k_{\mathrm{D5'}}}{k_{\mathrm{E}} + k_{\mathrm{D5'}}}$$

The subscript max implies $[\mathrm{I}] \gg K_{\mathrm{IE}}^{-1}$, not saturation of replication complexes with NTP substrate as would pertain to a Michaelis–Menten steady state with $[\mathrm{NTP}] \gg K_{\mathrm{m}}$ (Biebricher et al., 1983). Additional unimolecular steps in the elongation process would be taken into account by including their rate constants in the harmonic mean in the denominator of the K_{IE} expression. For concentrations and rate constants of present experiments, $K_{\mathrm{IE}}^{-1} \ll [\mathrm{I}]$ and $k_{\mathrm{D5'}} \ll k_{\mathrm{E}}$, so that

$$\mathrm{d}[\mathrm{I}]/\mathrm{d}t \rightarrow v_{\max} \qquad [\mathrm{E_c}] \rightarrow [\mathrm{E_0}] \qquad v_{\max} \rightarrow k_{\mathrm{D5'}}[\mathrm{E_0}]$$

$$K_{\mathrm{IE}} \rightarrow k_{\mathrm{A3'}}/k_{\mathrm{D5'}} \qquad \rho \rightarrow k_{\mathrm{D5'}}$$

Exponential Growth Solution. The rate constant matrix is

$$K = \begin{vmatrix} -k_{\mathrm{A3'}}[\mathrm{E}] & k_{\mathrm{E}} & k_{\mathrm{D5'}} \\ k_{\mathrm{A3'}}[\mathrm{E}] & -k_{\mathrm{E}} & 0 \\ 0 & k_{\mathrm{E}} & -k_{\mathrm{D5'}} \end{vmatrix}$$

and the characteristic equation is

$$\kappa^3 + (k_{\mathrm{A3'}}[\mathrm{E}] + k_{\mathrm{E}} + k_{\mathrm{D5'}})\kappa^2 + k_{\mathrm{D5'}}(k_{\mathrm{A3'}}[\mathrm{E}] + k_{\mathrm{E}})\kappa - k_{\mathrm{A3'}}[\mathrm{E}]k_{\mathrm{E}}k_{\mathrm{D5'}} = 0$$

Solution of quadratic approximation (equivalent to assuming the fastest step being equilibrated) gives

$$\kappa = \frac{k_{\mathrm{A3'}}[\mathrm{E}] + k_{\mathrm{E}}}{k_{\mathrm{A3'}}[\mathrm{E}] + k_{\mathrm{E}} + k_{\mathrm{D5'}}}\left(\left[\frac{k_{\mathrm{D5'}}^2}{4} + \frac{k_{\mathrm{A3'}}[\mathrm{E}]k_{\mathrm{E}}k_{\mathrm{D5'}}(k_{\mathrm{A3'}}[\mathrm{E}] + k_{\mathrm{E}} + k_{\mathrm{D5'}})}{(k_{\mathrm{A3'}}[\mathrm{E}] + k_{\mathrm{E}})^2}\right]^{1/2} - \frac{k_{\mathrm{D5'}}}{2}\right)$$

with limiting forms

$$\kappa \rightarrow k_{\mathrm{A3'}}[\mathrm{E}] \text{ as } [\mathrm{E}] \rightarrow 0 \text{ (not approached experimentally)}$$

$$\kappa \rightarrow \frac{k_{\mathrm{D5'}}}{2}[(1 + 4k_{\mathrm{E}}/k_{\mathrm{D5'}})^{1/2} - 1] \text{ as } [\mathrm{E}] \rightarrow \infty$$

The enzyme concentration at which $\kappa = (1/2)\kappa([\mathrm{E}] \rightarrow \infty)$ is

$$[\mathrm{E}]_{1/2} = \frac{k_{\mathrm{E}}}{k_{\mathrm{A3'}}}\left[\frac{1 + 2(k_{\mathrm{D5'}}/k_{\mathrm{E}})^{1/2}}{3 - 2(k_{\mathrm{D5'}}/k_{\mathrm{E}})^{1/2}}\right]$$

Concentration ratios in exponential growth phase are

$$\frac{[{}_1\mathrm{IE}]}{[\mathrm{I_0}]} = \frac{\kappa}{k_{\mathrm{E}}} \qquad \frac{[{}_n\mathrm{IE}]}{[\mathrm{I_0}]} = \frac{\kappa}{\kappa + k_{\mathrm{D5'}}} \qquad \frac{[\mathrm{I}]}{[\mathrm{I_0}]} = \frac{\kappa(\kappa + k_{\mathrm{E}})}{k_{\mathrm{E}}k_{\mathrm{A3'}}[\mathrm{E}]}$$

$$K_{\mathrm{IE}} = k_{\mathrm{A3'}}\frac{\kappa + k_{\mathrm{D5'}} + k_{\mathrm{E}}}{(\kappa + k_{\mathrm{E}})(\kappa + k_{\mathrm{D5'}})}$$

Computation of Rate Constants from Experimental Measurements. Combining ρ measured in the linear growth phase with the $[\mathrm{E}] \rightarrow \infty$ value of κ for the exponential growth phase gives

$$k_{\mathrm{D5'}} = \frac{1}{2}\kappa\left[\left(\frac{\kappa + 3\rho}{\kappa - \rho}\right)^{1/2} - 1\right]$$

$$k_{\mathrm{E}} = \frac{k_{\mathrm{D5'}}\rho}{k_{\mathrm{D5'}} - \rho}$$

The value of $k_{\mathrm{A3'}}$ can be determined by measuring the rate of complex formation from free I and E.

Selective values are

$$\sigma \approx \frac{1}{[\mathrm{I}]}\frac{\mathrm{d}[\mathrm{I}]}{\mathrm{d}t} = \begin{cases} \kappa & \text{(exponential phase)} \\ \dfrac{v_{\max}}{K_{\mathrm{IE}}^{-1} + [\mathrm{I}]} = k_{\mathrm{A3'}}[\mathrm{E}] & \text{(linear phase)} \end{cases}$$

New mutants can grow out when wild type is in the linear growth phase if [E] is large enough to permit κ of mutant to exceed σ of wild type. At NTP concentrations lower than required to saturate the replication complexes, $v_{\max}$ in the above equations becomes v (Biebricher et al., 1983).

(II) Kinetics for Three-Step Replication Mechanism at CSTR Steady State

Kinetic Equations. To the kinetic equations in Appendix I are added the dilution terms $-k_{\mathrm{DIL}}[\mathrm{I}]$, $+k_{\mathrm{DIL}}([\mathrm{E}]_{\mathrm{in}} - [\mathrm{E}])$, $-k_{\mathrm{DIL}}[{}_1\mathrm{IE}]$, and $-k_{\mathrm{DIL}}[{}_n\mathrm{IE}]$ where $[\mathrm{E}]_{\mathrm{in}}$ is the concentration of enzyme in the input stream.

Flow Steady-State Concentrations. These are defined as follows:

$$[\mathrm{I}]_{\mathrm{ss}} = \{[\mathrm{E}]_{\mathrm{in}}[k_{\mathrm{E}}k_{\mathrm{D5'}} - k_{\mathrm{DIL}}(k_{\mathrm{D5'}} + k_{\mathrm{DIL}})] - (k_{\mathrm{DIL}}/k_{\mathrm{A3'}})(k_{\mathrm{D5'}} + k_{\mathrm{DIL}})(k_{\mathrm{E}} + k_{\mathrm{DIL}})\}/\{(k_{\mathrm{D5'}} + k_{\mathrm{DIL}})(k_{\mathrm{E}} + k_{\mathrm{DIL}}) - k_{\mathrm{E}}k_{\mathrm{D5'}}\}$$

$$[\mathrm{E}]_{\mathrm{ss}} = \frac{k_{\mathrm{DIL}}(k_{\mathrm{DIL}} + k_{\mathrm{D5'}})(k_{\mathrm{DIL}} + k_{\mathrm{E}})}{k_{\mathrm{A3'}}[k_{\mathrm{E}}k_{\mathrm{D5'}} - k_{\mathrm{DIL}}(k_{\mathrm{DIL}} + k_{\mathrm{D5'}})]} < [\mathrm{E}]_{\mathrm{in}}$$

$$[{}_1\mathrm{IE}]_{\mathrm{ss}} = \frac{k_{\mathrm{A3'}}[\mathrm{I}][\mathrm{E}]}{k_{\mathrm{E}} + k_{\mathrm{DIL}}}$$

$$[{}_n\mathrm{IE}]_{\mathrm{ss}} = \frac{k_{\mathrm{A3'}}k_{\mathrm{E}}[\mathrm{I}][\mathrm{E}]}{(k_{\mathrm{D5'}} + k_{\mathrm{DIL}})(k_{\mathrm{E}} + k_{\mathrm{DIL}})}$$

$$K_{\mathrm{IE}} = \frac{k_{\mathrm{A3'}}(k_{\mathrm{E}} + k_{\mathrm{D5'}} + k_{\mathrm{DIL}})}{(k_{\mathrm{D5'}} + k_{\mathrm{DIL}})(k_{\mathrm{E}} + k_{\mathrm{DIL}})}$$

where the inequality in the $[\mathrm{E}]_{\mathrm{ss}}$ equation requires that k_{DIL}

must be small enough to ensure that the denominator does not become so small that [E] is predicted to exceed the input concentration $[\mathrm{E}]_{\mathrm{in}}$. Comparing [E] to $[\mathrm{E}]_{\mathrm{in}}$ provides a measure of whether the RNA synthesis rate is fast enough to compete with the flow rate.

Approach to Flow Steady State. If the flow experiment is started with an RNA concentration $[\mathrm{I}]_{t=0}$ much smaller than the enzyme concentration $[\mathrm{E}]_{\mathrm{in}}$, the growth of [I] follows

$$[\mathrm{I}] = [\mathrm{I}]_{t=0} \exp[(\kappa - k_{\mathrm{DIL}})t]$$

at first, where κ is as given in Appendix I. If at $t = 0$ the RNA concentration is high enough to saturate the enzyme, then before the flow steady state is established steady-state concentrations of the replication complexes may be established, such that

$$[{}_n\mathrm{IE}] = \frac{k_{\mathrm{E}}[{}_1\mathrm{IE}]}{k_{\mathrm{D5'}} + k_{\mathrm{DIL}}} \qquad [{}_1\mathrm{IE}] = \frac{k_{\mathrm{A3'}}[\mathrm{E}][\mathrm{I}]}{k_{\mathrm{E}} + k_{\mathrm{DIL}}}$$

and the free enzyme concentration is given by

$$[\mathrm{E}] = \frac{(k_{\mathrm{D5'}} + k_{\mathrm{DIL}})(k_{\mathrm{E}} + k_{\mathrm{DIL}})[\mathrm{E}]_{\mathrm{in}}}{(k_{\mathrm{D5'}} + k_{\mathrm{DIL}})(k_{\mathrm{E}} + k_{\mathrm{DIL}}) + k_{\mathrm{A3'}}(k_{\mathrm{E}} + k_{\mathrm{D5'}} + k_{\mathrm{DIL}})[\mathrm{I}]}$$

The kinetic equation for [I] is then

$$\frac{\mathrm{d}[\mathrm{I}]}{\mathrm{d}t} = \left[\frac{k_{\mathrm{A3'}}[k_{\mathrm{E}}k_{\mathrm{D5'}} - k_{\mathrm{DIL}}(k_{\mathrm{D5'}} + k_{\mathrm{DIL}})][\mathrm{E}]_{\mathrm{in}}}{(k_{\mathrm{E}} + k_{\mathrm{DIL}})(k_{\mathrm{D5'}} + k_{\mathrm{DIL}}) + k_{\mathrm{A3'}}(k_{\mathrm{E}} + k_{\mathrm{D5'}} + k_{\mathrm{DIL}})[\mathrm{I}]} - k_{\mathrm{DIL}}\right][\mathrm{I}] = \frac{a[\mathrm{I}]}{b + c[\mathrm{I}]} - k_{\mathrm{DIL}}[\mathrm{I}]$$

If at $t = 0$ the $c[\mathrm{I}]$ and $k_{\mathrm{DIL}}[\mathrm{I}]$ terms can be neglected, the approach to the flow steady state begins exponentially:

$$[\mathrm{I}] = [\mathrm{I}]_{t=0}e^{at/b}$$

If at $t = t_1$ $c[\mathrm{I}] \gg b$ but $k_{\mathrm{DIL}}[\mathrm{I}]$ can still be neglected, the approach to the flow steady state proceeds linearly:

$$[\mathrm{I}] = [\mathrm{I}]_{t=t_1} + (a/c)(t - t_1)$$

At long times $t > t_2$ the $k_{\mathrm{DIL}}[\mathrm{I}]$ term governs the exponential approach to the final flow steady state:

$$[\mathrm{I}] = \frac{a}{ck_{\mathrm{DIL}}} - \left(\frac{a}{ck_{\mathrm{DIL}}} - [\mathrm{I}]_{t_2}\right)e^{-k_{\mathrm{DIL}}(t-t_2)}$$

Effect of Double-Strand Formation. Addition of $-(1/2)k_{\mathrm{ds}}[\mathrm{I}]^2$ (Appendix III) to the kinetic equation for [I] leads to a free enzyme concentration given by positive roots of

$$[\mathrm{E}]\left(\left[1 - \frac{k_{\mathrm{E}}k_{\mathrm{D5'}}}{(k_{\mathrm{D5'}} + k_{\mathrm{DIL}})(k_{\mathrm{E}} + k_{\mathrm{DIL}})}\right]\left[k_{\mathrm{DIL}} - \frac{k_{\mathrm{A3'}}[\mathrm{E}][k_{\mathrm{E}}k_{\mathrm{D5'}} - k_{\mathrm{DIL}}(k_{\mathrm{D5'}} + k_{\mathrm{DIL}})]}{(k_{\mathrm{D5'}} + k_{\mathrm{DIL}})(k_{\mathrm{E}} + k_{\mathrm{DIL}})}\right] + \frac{k_{\mathrm{ds}}k_{\mathrm{DIL}}}{2k_{\mathrm{A3'}}}\right) - \frac{k_{\mathrm{ds}}k_{\mathrm{DIL}}[\mathrm{E}]_{\mathrm{in}}}{2k_{\mathrm{A3'}}} = 0$$

(*III*) *Concentrations When Double-Strand Formation Is at Steady State*

The kinetic equation for [I] $(=[\mathrm{I}^+] + [\mathrm{I}^-])$ in Appendix I must be changed to account for double-strand formation by including the term $-(1/2)k_{\mathrm{ds}}[\mathrm{I}]^2$. The kinetic equation for double strand is

$$\mathrm{d}[\mathrm{II}]/\mathrm{d}t = (1/4)k_{\mathrm{ds}}[\mathrm{I}]^2$$

Setting the derivatives of [I], $[{}_1\mathrm{IE}]$, and $[{}_n\mathrm{IE}]$ to zero and requiring $[\mathrm{E}_0] = [\mathrm{E}] + [{}_1\mathrm{IE}] + [{}_n\mathrm{IE}]$ lead to

$$[\mathrm{E}] = \frac{k_{\mathrm{ds}}}{4k_{\mathrm{A3'}}K_{\mathrm{IE}}}\left(\left[\frac{8[\mathrm{E}_0]k_{\mathrm{A3'}}K_{\mathrm{IE}}}{k_{\mathrm{ds}}} + 1\right]^{1/2} - 1\right)$$

$$K_{\mathrm{IE}} = \frac{k_{\mathrm{A3'}}(k_{\mathrm{E}} + k_{\mathrm{D5'}})}{k_{\mathrm{E}}k_{\mathrm{D5'}}} \qquad [\mathrm{I}] = 2\frac{k_{\mathrm{A3'}}}{k_{\mathrm{ds}}}[\mathrm{E}] = (2v/k_{\mathrm{ds}})^{1/2}$$

$$[{}_1\mathrm{IE}] = 2\frac{k_{\mathrm{A3'}}{}^2}{k_{\mathrm{ds}}k_{\mathrm{E}}}[\mathrm{E}]^2 \qquad [{}_n\mathrm{IE}] = 2\frac{k_{\mathrm{A3'}}{}^2}{k_{\mathrm{ds}}k_{\mathrm{D5'}}}[\mathrm{E}]^2$$

$$[\mathrm{E_c}] = 2\frac{k_{\mathrm{A3'}}K_{\mathrm{IE}}}{k_{\mathrm{ds}}}[\mathrm{E}]^2 \qquad v = \frac{k_{\mathrm{E}}k_{\mathrm{D5'}}}{k_{\mathrm{E}} + k_{\mathrm{D5'}}}[\mathrm{E_c}] = \rho[\mathrm{E_c}]$$

The only growing concentration is [II], which follows

$$\frac{\mathrm{d}[\mathrm{II}]}{\mathrm{d}t} = \frac{v}{2} = \frac{\rho[\mathrm{E_c}]}{2} = \frac{k_{\mathrm{A3'}}[\mathrm{E_c}]}{2K_{\mathrm{IE}}} = \frac{k_{\mathrm{A3'}}{}^2}{k_{\mathrm{ds}}}[\mathrm{E}]^2$$

(*IV*) *Coexistence of Two Species When Double-Strand Formation Is at Steady State*

The steady-state equations of Appendix III hold for both species ${}^1\mathrm{I}$ and ${}^2\mathrm{I}$, with the enzyme conservation equation being

$$[\mathrm{E}_0] = [\mathrm{E}] + [{}^1_1\mathrm{IE}] + [{}^2_1\mathrm{IE}] + [{}^1_n\mathrm{IE}] + [{}^2_n\mathrm{IE}]$$

Defining

$$x = \frac{{}^1k_{\mathrm{A3'}}}{{}^1K_{\mathrm{IE}}{}^{11}k_{\mathrm{ds}}} + \frac{{}^2k_{\mathrm{A3'}}}{{}^2K_{\mathrm{IE}}{}^{22}k_{\mathrm{ds}}}$$

and

$${}^iK_{\mathrm{IE}} = [{}^i\mathrm{E_c}]/([{}^i\mathrm{I}][\mathrm{E}])$$

the steady-state enzyme concentration is

$$[\mathrm{E}] = [(8[\mathrm{E}_0]x + 1)^{1/2} - 1]/(4x)$$

The other concentrations are related to [E] as in Appendix III. From them we can derive the ratios

$$\frac{[{}^2\mathrm{I}]}{[{}^1\mathrm{I}]} = \frac{{}^2k_{\mathrm{A3'}}{}^{11}k_{\mathrm{ds}}}{{}^1k_{\mathrm{A3'}}{}^{22}k_{\mathrm{ds}}} \qquad \frac{[{}^2_1\mathrm{IE}]}{[{}^1_1\mathrm{IE}]} = \frac{({}^2k_{\mathrm{A3'}})^2\,{}^1k_{\mathrm{E}}{}^{11}k_{\mathrm{ds}}}{({}^1k_{\mathrm{A3'}})^2\,{}^2k_{\mathrm{E}}{}^{22}k_{\mathrm{ds}}}$$

$$\frac{[{}^2_n\mathrm{IE}]}{[{}^1_n\mathrm{IE}]} = \frac{({}^2k_{\mathrm{A3'}})^2\,{}^{11}k_{\mathrm{ds}}{}^1k_{\mathrm{D5'}}}{({}^1k_{\mathrm{A3'}})^2\,{}^{22}k_{\mathrm{ds}}{}^2k_{\mathrm{D5'}}} \qquad \frac{[{}^2\mathrm{E_c}]}{[{}^1\mathrm{E_c}]} = \frac{{}^2K_{\mathrm{IE}}{}^2k_{\mathrm{A3'}}{}^{11}k_{\mathrm{ds}}}{{}^1K_{\mathrm{IE}}{}^1k_{\mathrm{A3'}}{}^{22}k_{\mathrm{ds}}}$$

$${}^iK_{\mathrm{IE}} = \frac{{}^ik_{\mathrm{A3'}}({}^ik_{\mathrm{E}} + {}^ik_{\mathrm{D5'}})}{{}^ik_{\mathrm{E}}{}^ik_{\mathrm{D5'}}}$$

The double-strand ratio changes according to

$$\frac{\mathrm{d}[{}^{22}\mathrm{II}]}{\mathrm{d}[{}^{11}\mathrm{II}]} = \frac{\mathrm{d}[{}^{22}\mathrm{II}]/\mathrm{d}t}{\mathrm{d}[{}^{11}\mathrm{II}]/\mathrm{d}t} = \frac{({}^2k_{\mathrm{A3'}})^2\,{}^{11}k_{\mathrm{ds}}}{({}^1k_{\mathrm{A3'}})^2\,{}^{22}k_{\mathrm{ds}}} = \text{constant}$$

meaning that after sufficient time ($t \rightarrow \infty$) the ratio of double-strand concentrations will remain constant; i.e., $[{}^{22}\mathrm{II}]/[{}^{11}\mathrm{II}]$ = constant or d ln $[{}^{22}\mathrm{II}]/\mathrm{d}t$ = d ln $[{}^{11}\mathrm{II}]/\mathrm{d}t$.

(*V*) *Coexistence of Hybridizing RNA Species*

Coexistence of two hybridizing RNAs ${}^1\mathrm{I}$ and ${}^2\mathrm{I}$ that form complementary double strands ${}^{11}\mathrm{II}$ and ${}^{22}\mathrm{II}$ as well as a hybrid double-strand ${}^{12}\mathrm{II}$ with rate constant ${}^{12}k_{\mathrm{ds}}$ (referring to each of the two elementary reactions ${}^1\mathrm{I}^+ + {}^2\mathrm{I}^- \rightarrow {}^{12}\mathrm{II}$ and ${}^1\mathrm{I}^- + {}^2\mathrm{I}^+ \rightarrow {}^{21}\mathrm{II}$) is possible if the inequalities given below are satisfied.

Adding the term $-(1/2){}^{12}k_{\mathrm{ds}}[{}^1\mathrm{I}][{}^2\mathrm{I}]$ to the kinetic equations for the sum concentrations $[{}^1\mathrm{I}]$ and $[{}^2\mathrm{I}]$ and setting to zero the time derivatives of the species concentration sums $[{}^1\mathrm{I}]$, $[{}^2\mathrm{I}]$, $[{}^1_1\mathrm{IE}]$, $[{}^2_1\mathrm{IE}]$, $[{}^1_n\mathrm{IE}]$, and $[{}^2_n\mathrm{IE}]$ lead under enzyme conservation according to $[\mathrm{E}_0] = [\mathrm{E}] + [{}^1_1\mathrm{IE}] + [{}^1_n\mathrm{IE}] + [{}^2_1\mathrm{IE}] + [{}^2_n\mathrm{IE}]$ to

$$\frac{[{}^{2}\mathrm{I}]}{[{}^{1}\mathrm{I}]} = \frac{{}^{2}k_{\mathrm{A3'}}{}^{11}k_{\mathrm{ds}} - {}^{1}k_{\mathrm{A3'}}{}^{12}k_{\mathrm{ds}}}{{}^{1}k_{\mathrm{A3'}}{}^{22}k_{\mathrm{ds}} - {}^{2}k_{\mathrm{A3'}}{}^{12}k_{\mathrm{ds}}}$$

$$[\mathrm{E}] = \frac{[8(\beta_1{}^{1}K_{\mathrm{IE}} + \beta_2{}^{2}K_{\mathrm{IE}})[\mathrm{E}_0] + 1]^{1/2} - 1}{4(\beta_2{}^{1}K_{\mathrm{IE}} + \beta_2{}^{2}K_{\mathrm{IE}})}$$

where

$$\beta_1 = \frac{{}^{1}k_{\mathrm{A3'}}{}^{22}k_{\mathrm{ds}} - {}^{2}k_{\mathrm{A3'}}{}^{12}k_{\mathrm{ds}}}{{}^{11}k_{\mathrm{ds}}{}^{22}k_{\mathrm{ds}} - {}^{12}k_{\mathrm{ds}}{}^{2}}$$

$$\beta_2 = \frac{{}^{2}k_{\mathrm{A3'}}{}^{11}k_{\mathrm{ds}} - {}^{1}k_{\mathrm{A3'}}{}^{12}k_{\mathrm{ds}}}{{}^{11}k_{\mathrm{ds}}{}^{22}k_{\mathrm{ds}} - {}^{12}k_{\mathrm{ds}}{}^{2}}$$

and the prefixed superscripts denote rate constants for each species.

The steady-state concentrations are

$$[{}^{1}\mathrm{I}] = 2\beta_1[\mathrm{E}] \qquad [{}^{2}\mathrm{I}] = 2\beta_2[\mathrm{E}] \qquad [{}^{1}_{1}\mathrm{IE}] = 2\beta_1\frac{{}^{1}k_{\mathrm{A3'}}}{{}^{1}k_{\mathrm{E}}}[\mathrm{E}]^2$$

$$[{}^{2}_{1}\mathrm{IE}] = 2\beta_2\frac{{}^{2}k_{\mathrm{A3'}}}{{}^{2}k_{\mathrm{E}}}[\mathrm{E}]^2 \qquad [{}^{1}_{n}\mathrm{IE}] = 2\beta_1\frac{{}^{1}k_{\mathrm{A3'}}}{{}^{1}k_{\mathrm{D5'}}}[\mathrm{E}]^2$$

$$[{}^{2}_{n}\mathrm{IE}] = 2\beta_2\frac{{}^{2}k_{\mathrm{A3'}}}{{}^{2}k_{\mathrm{D5'}}}[\mathrm{E}]^2$$

For all concentrations to be positive, β_1 and β_2 must both be positive. The only stable coexistence of two species is derived from this condition to be defined by the inequalities

$${}^{11}k_{\mathrm{ds}}{}^{22}k_{\mathrm{ds}} > {}^{22}k_{\mathrm{ds}}{}^{12}k_{\mathrm{ds}}({}^{1}k_{\mathrm{A3'}}/{}^{2}k_{\mathrm{A3'}}) > {}^{12}k_{\mathrm{ds}}{}^{2}$$

Violation of either inequality implies extinction of one species. If the inequalities are satisfied, species 2 predominates at coexistence when the expression

$$\frac{{}^{2}k_{\mathrm{A3'}}}{{}^{1}k_{\mathrm{A3'}}} - \frac{1 + {}^{22}k_{\mathrm{ds}}/{}^{12}k_{\mathrm{ds}}}{1 + {}^{11}k_{\mathrm{ds}}/{}^{12}k_{\mathrm{ds}}}$$

is positive. The production rates are

$$\mathrm{d}[{}^{12}\mathrm{II}]/\mathrm{d}t = (1/2){}^{12}k_{\mathrm{ds}}\beta_1\beta_2[\mathrm{E}]^2$$

$$\mathrm{d}[{}^{11}\mathrm{II}]/\mathrm{d}t = {}^{11}k_{\mathrm{ds}}\beta_1{}^{2}[\mathrm{E}]^2 \qquad \mathrm{d}[{}^{22}\mathrm{II}]/\mathrm{d}t = {}^{22}k_{\mathrm{ds}}\beta_2{}^{2}[\mathrm{E}]^2$$

Registry No. RNA replicase, 9026-28-2.

REFERENCES

Batschelet, E., Domingo, E., & Weissman, C. (1976) *Gene 1*, 27–32.

Biebricher, C. K. (1983) *Evol. Biol. 16*, 1–52.

Biebricher, C. K., Eigen, M., & Luce, R. (1981a) *J. Mol. Biol. 148*, 369–390.

Biebricher, C. K., Eigen, M., & Luce, R. (1981b) *J. Mol. Biol. 148*, 391–410.

Biebricher, C. K., Diekmann, S., & Luce, R. (1982) *J. Mol. Biol. 154*, 629–648.

Biebricher, C. K., Eigen, M., & Gardiner, W. C., Jr. (1983) *Biochemistry 22*, 2544–2559.

Biebricher, C. K., Eigen, M., & Gardiner, W. C., Jr. (1984) *Biochemistry 23*, 3186–3194.

Eigen, M. (1971) *Naturwissenschaften 58*, 465–523.

Eigen, M., & Winkler-Oswatitsch, R. (1973) in *Mannheimer Forum 1973/4*, pp 53–139, Studienreihe Boehringer, Mannheim, West Germany.

Eigen, M., & Winkler-Oswatitsch, R. (1975) *Das Spiel*, Piper, Munich.

Eigen, M., & Schuster, P. (1977) *Naturwissenschaften 64*, 541–565.

Kramer, F. R., Mills, D. R., Cole, P. E., Nishihara, T., & Spiegelman, S. (1974) *J. Mol. Biol. 89*, 719–736.

Küppers, B.-O. (1979) *Naturwissenschaften 66*, 228–243.

Mills, D. R., Peterson, R. L., & Spiegelman, S. (1967) *Proc. Natl. Acad. Sci. U.S.A. 58*, 217–224.

Mills, D. R., Dobkin, C., & Kramer, F. R. (1978) *Cell (Cambridge, Mass.) 15*, 541–550.

Sumper, M., & Luce, R. (1975) *Proc. Natl. Acad. Sci. U.S.A. 72*, 162–166.

Wetmur, J. G., & Davidson, N. (1968) *J. Mol. Biol. 31*, 349–370.